CP Violation in the B^0 meson system with BaBar

James Weatherall (representing the *BABAR* Collaboration)

Department of Physics and Astronomy, University of Manchester,
Oxford Road, Manchester, M13 9PL, UK

The *BABAR* detector, at the PEP-II asymmetric B Factory at SLAC collected a sample of 32 million $B\overline{B}$ pairs whilst operating at energies near the $\Upsilon(4S)$ resonance between October 1999 and May 2001. A study of time-dependent CP-violating asymmetries in events where one neutral B meson is fully reconstructed in a final state containing charmonium produced the measurement $\sin 2\beta = 0.59 \pm 0.14\,(\mathrm{stat}) \pm 0.05\,(\mathrm{syst})$, which constitutes an observation of CP violation in the B^0 meson system at the 4σ level. Also presented are preliminary results from a study of CP violation in the decays $B^0 \to \pi^+\pi^-$ and $B^0 \to K^+\pi^-$.

1. Introduction

CP violation was first observed in the decays of K^0_L mesons in 1964 [1]. It was 37 years before this phenomenon was observed in another system, that of the neutral B mesons. The effect arises from the existence of an irremovable, CP-violating phase in the three-generation CKM quark-mixing matrix [2]. The B^0 system has an important advantage over the K^0 system in that the measurements of CP-violating asymmetries provide a direct test of the Standard Model of electroweak interactions, free of corrections from strong interactions, which arise when trying to interpret the results from K^0_L decays. The primary goal of *BABAR* is to over-constrain the Unitarity Triangle through multiple, independent measurements of its sides and angles. In this analysis, the angle β is probed through a measurement of $\sin 2\beta$ using $b \to c\bar{c}s$ decays.

2. PEP-II and *BABAR*

The PEP-II B factory at SLAC comprises a pair of storage rings producing asymmetric e^+e^- collisions ($9\,\mathrm{GeV}$ e^-, $3.1\,\mathrm{GeV}$ e^+) at a center-of-mass energy corresponding to the mass of the $\Upsilon(4S)$ resonance ($10.58\,\mathrm{GeV}$). The $\Upsilon(4S)$ decays almost exclusively to B^+B^- or coherent $B^0\overline{B}^0$ pairs. The primary goal of the *BABAR* detector for this analysis is to measure the time difference between the two meson decays, Δt. The asymmetric nature of the collisions gives a boost of $\beta\gamma = 0.55$ which yields an average spatial vertex separation of $\approx 250\,\mu\mathrm{m}$.

A detailed description of the *BABAR* detector can be found in [3]. The volume inside the 1.5T superconducting solenoid consists of a five layer silicon vertex detector (SVT), a drift chamber (DCH), a quartz Cerenkov detector (DIRC) and a CsI(Tl) crystal electromagnetic calorimeter (EMC). The instrumented flux return (IFR) outside the magnet comprises alternate layers of iron and resistive plate counters (RPCs).

3. Exclusive B reconstruction

A sample of neutral B mesons, B_{CP} have been fully reconstructed in their decays to final states of known CP content: $J/\psi K^0_S$, $\psi(2S)K^0_S$, $J/\psi K^0_L$, $\chi_{c1}K^0_S$ and $J/\psi K^{*0}(K^{*0} \to K^0_S\pi^0)$. In addition there are also samples of B decays to final states of definite flavour (B_{flav}): $B^0 \to D^{(*)-}\pi^+$, $D^{(*)-}\rho^+$, $D^{(*)-}a_1^+$ and $J/\psi K^{*0}(K^{*0} \to K^+\pi^-)$ as well as charged B decays: $B^- \to D^{(*)0}\pi^-$, $J/\psi K^-$ and $\psi(2S)K^-$ (charge conjugate modes are implied throughout this paper). All selections have been optimized to give maximum sensitivity to the final measurement. Particle identification, mass (or mass difference) and vertex constraints are used wherever applicable. The resulting signal yield for each mode is identified by using the kinematical variables $\Delta E = E_B^* - E_{beam}^*$ and $m_{ES} = \sqrt{E_{beam}^{*2} - p_B^{*2}}$ where E_B^*, p_B^* are the center-of-mass energy and momentum of the reconstructed B and E_{beam}^* is the beam energy in the center-of-mass. In the case that an event has more than one B candidate, only the one with the smallest $|\Delta E|$ is retained. For each mode a signal region is defined as $\pm 3\sigma$ about (5.279,0) in the $m_{ES}, \Delta E$ plane. The m_{ES} resolution is $\approx 3\,\mathrm{MeV}/c^2$, dominated by the spread of the beam energy. The ΔE resolution is mode dependent and varies from about 10-33 MeV. Figure 1 shows the m_{ES} distributions for B_{CP} candidates containing a K_S^0 and the ΔE distribution for candidates containing a K_L^0. The number of tagged events and the signal purities, determined from fits to the m_{ES} (all K_S^0 modes except K^{*0}) or ΔE (K_L^0 mode) distributions in data or from Monte Carlo simulation (K^{*0} mode) are shown in table 1.

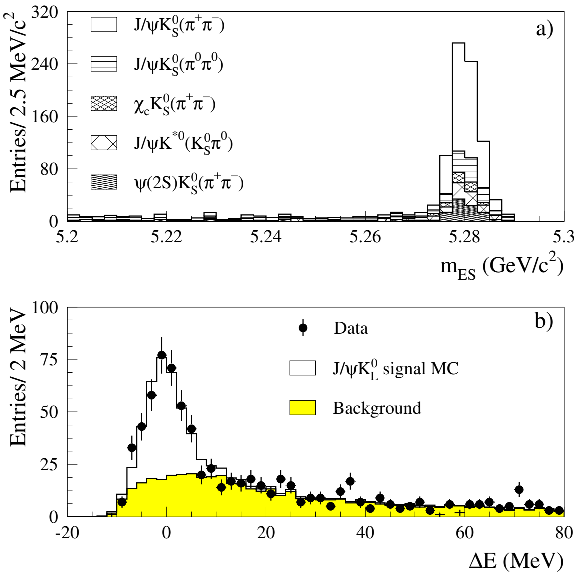

Figure 1. a) Distribution of m_{ES} for B_{CP} candidates having a K_S^0 in the final state; b) distribution of ΔE for $J/\psi K_L^0$ candidates.

4. Flavour Tagging

Flavour tagging information is extracted from the other (partially reconstructed) B in the event, $B_{\rm tag}$. The coherent production of the $B^0\overline{B}^0$ pair ensures that the flavour of B_{CP} is exactly opposite to that of $B_{\rm tag}$ at the time when $B_{\rm tag}$ decays, t_{tag}. Each event is assigned to one of four hierarchical, mutually exclusive tagging categories or excluded from further analysis. The `Lepton` and `Kaon` categories contain events with high momentum leptons from semileptonic B decays or with kaons whose charge is correlated with the flavour of the decaying b quark (e.g. a positive lepton or kaon yields a B^0 tag). The `NT1` and `NT2` categories are based on a neural network algorithm whose tagging power arises primarily from soft pions from D^{*+} decays and from recovering unidentified isolated primary leptons. The $B_{\rm flav}$ sample is used to measure the tagging performance along with the B_{CP} events. The figure of merit used is $Q_i = \epsilon_i(1-2w_i)^2$ where ϵ_i and w_i are the efficiency and mistag fraction for category i. The statistical error on $\sin 2\beta$ is proportional to $1/\sqrt{Q}$, where $Q = \sum Q_i$. The efficiencies and mistag fractions for the four tagging categories are shown in table 2.

Table 2
Efficiencies ϵ_i and average mistag fractions w_i extracted for each tagging category i from a maximum likelihood fit to the time distribution for the fully reconstructed B sample ($B_{CP} + B_{\rm flav}$). Uncertainties are statistical only.

Category	$\epsilon(\%)$	$w(\%)$	$Q(\%)$
`Lepton`	10.9 ± 0.3	8.9 ± 1.3	7.4 ± 0.5
`Kaon`	35.8 ± 0.5	17.6 ± 1.0	15.0 ± 0.9
`NT1`	7.8 ± 0.3	22.0 ± 2.1	2.5 ± 0.4
`NT2`	13.8 ± 0.3	35.1 ± 1.9	1.2 ± 0.3
All	68.4 ± 0.7		26.1 ± 1.2

5. Δt measurement and resolution

The time difference between the two B decays, $\Delta t = t_{CP} - t_{tag}$ is determined by first measuring

Table 1
Number of tagged events, signal purity and result of fitting for *CP* asymmetries in the full *CP* sample and in various subsamples, as well as in the $B_{\rm flav}$ and charged B control samples. Errors are statistical only.

Sample	$N_{\rm tag}$	Purity (%)	$\sin 2\beta$
$J/\psi K^0_S$,$\psi(2S)K^0_S$,$\chi_{c1}K^0_S$	480	96	0.56 ± 0.15
$J/\psi K^0_L$ ($\eta_f = +1$)	273	51	0.70 ± 0.34
$J/\psi K^{*0}, K^{*0} \to K^0_S\pi^0$	50	74	0.82 ± 1.00
Full *CP* sample	803	80	0.59 ± 0.14
$J/\psi K^0_S$, $\psi(2S)K^0_S$, $\chi_{c1}K^0_S$ only ($\eta_f = -1$)			
$J/\psi K^0_S$ ($K^0_S \to \pi^+\pi^-$)	316	98	0.45 ± 0.18
$J/\psi K^0_S$ ($K^0_S \to \pi^0\pi^0$)	64	94	0.70 ± 0.50
$\psi(2S)K^0_S$ ($K^0_S \to \pi^+\pi^-$)	67	98	0.47 ± 0.42
$\chi_{c1}K^0_S$ ($K^0_S \to \pi^+\pi^-$)	33	97	$2.59 \pm ^{0.55}_{0.67}$
`Lepton` tags	74	100	0.54 ± 0.29
`Kaon` tags	271	98	0.59 ± 0.20
`NT1` tags	46	97	0.67 ± 0.45
`NT2` tags	89	95	0.10 ± 0.74
B^0 tags	234	98	0.50 ± 0.22
$\overline{B}^0$ tags	246	97	0.61 ± 0.22
$B_{\rm flav}$ non-*CP* sample	7591	86	0.02 ± 0.04
Charged B non-*CP* sample	6814	86	0.03 ± 0.04

their spatial separation $\Delta z = z_{CP} - z_{tag}$. This is corrected on an event-by-event basis for the direction of the B with respect to the z direction in the $\Upsilon(4S)$ frame. z_{CP} is determined from the charged tracks that constitute the B_{CP} candidate. All other tracks in the event are fitted to a common vertex in order to calculate the $B_{\rm tag}$ decay position, z_{tag}. Tracks from photon conversions are removed. Pairs of tracks compatible with the decay of a long lived K^0_S or Λ are replaced by their parent neutral pseudotrack. The bias in the forward z direction due to charm decays is reduced by removing the track with the largest contribution to the vertex χ^2, if above 6 and iterating the fit until either no track fulfills this condition or fewer than two tracks remain. Knowledge of the beam spot location and beam direction is incorporated through the addition of a pseudotrack to the tagging vertex, computed from the $B_{CP}(B_{\rm flav})$ vertex and three-momentum, the beam spot (with a vertical size of 10 μm) and the $\Upsilon(4S)$ momentum. The total Δz reconstruction efficiency is 97%. For 99% of the reconstructed vertices the r.m.s. Δz resolution is 180 μm, dominated by the $B_{\rm tag}$ vertex. An accepted candidate must have a converged fit for the B_{CP} and $B_{\rm tag}$ vertices, an error of less than 400 μm on Δz and a measured $|\Delta t| < 20$ ps.

The Δt resolution function for signal events is represented as a sum of three Gaussian distributions. All offsets are modelled to be proportional to the event-by-event error, $\sigma_{\Delta t}$, which is correlated with the weight that the daughters of long-lived charm particles have in the tag vertex reconstruction. The 'core' and 'tail' Gaussians have widths scaled by the event-by-event measurement error derived from the vertex fits. A separate offset for the core distribution is allowed for each tagging category to account for small shifts caused by inclusion of residual charm decay products in the tag vertex. The third Gaussian has a fixed width of 8 ps and accounts for fewer than 1% of events with incorrectly reconstructed vertices. Identical resolution function parameters are used for all modes, since the Δt resolution is dominated by the $B_{\rm tag}$ vertex precision. Separate resolution function parameters have been used for data collected in 1999-2000 and 2001, due to the significant improvement in the SVT alignment.

6. Measuring $\sin 2\beta$

6.1. Improvements to the analysis

There are several significant changes in this analysis [4] relative to the first *BABAR* $\sin 2\beta$ publication [5]. The B_{CP} modes $\chi_{c1} K^0_S$ and $J/\psi K^{*0} (K^{*0} \to K^0_S \pi^0)$ have been added. Improvements in track and K^0_S reconstruction efficiency in 2001 data produce a $\approx 30\%$ increase in the yields per luminosity unit. Better alignment of the tracking systems in 2001 data and improvements in the tag vertex reconstruction algorithm have increased the sensitivity of the measurement by an additional 10%. The purity of the sample has been increased by a reoptimization of the $J/\psi K^0_L$ selection. In total, the statistical power of the analysis is almost doubled with respect to that of Ref. [5]. The final B_{CP} sample contains about 640 events, the $B_{\rm flav}$ sample has 7591 fully reconstructed B^0 events and the charged B sample has 6814 fully reconstructed $B^{\pm}$ events.

6.2. The $\sin 2\beta$ fit

The fit for $\sin 2\beta$ is based on the following framework. Each event in the B_{CP} sample is examined for evidence that the $B_{\rm tag}$ decayed as a B^0 or $\overline{B}^0$. The decay distributions as a function of time for events with either type of tag can be expressed in terms of a complex parameter λ that depends both on $B^0 \overline{B}^0$ mixing and the amplitudes describing B^0 and $\overline{B}^0$ decay to a common final state f [6]. The distribution $\mathrm{f}_+ (\mathrm{f}_-)$ of the decay rate when the tag is a $B^0 (\overline{B}^0)$ is

$$\mathrm{f}_\pm(\Delta t) = \frac{\mathrm{e}^{-|\Delta t|/\tau_{B^0}}}{2\tau_{B^0}(1+|\lambda|^2)} \times \left[\frac{1+|\lambda|^2}{2} \right. \\ \left. \pm\, \mathcal{I}m\lambda \sin(\Delta m_{B^0} \Delta t) \mp \frac{1-|\lambda|^2}{2} \cos(\Delta m_{B^0} \Delta t) \right],$$

where τ_{B^0} is the B^0 lifetime and ΔM_{B^0} is the oscillation frequency of $B^0 \overline{B}^0$ mixing. The first oscillatory term is due to interference between direct decay and decay after mixing. A difference between the B^0 and $\overline{B}^0$ Δt distributions or a Δt asymmetry for either flavour tag is evidence for *CP* violation.

In the Standard Model, $\lambda = \eta_f e^{-2i\beta}$ for $b \to c\overline{c}s$ decays containing charmonium where η_f is the *CP* eigenvalue of the state f and $\beta = \arg[-V_{cd}V^*_{cb}/-V_{td}V^*_{tb}]$ is an angle of the Unitarity Triangle. Thus, the time-dependent *CP*-violating asymmetry is

$$A_{CP}(\Delta t) \equiv \frac{\mathrm{f}_+(\Delta t) - \mathrm{f}_-(\Delta t)}{\mathrm{f}_+(\Delta t) + \mathrm{f}_-(\Delta t)} \\ = -\eta_f \sin 2\beta \sin(\Delta m_{B^0}\, \Delta t),$$

where $\eta_f = -1$ for $J/\psi K^0_S$, $\psi(2S) K^0_S$ and $\chi_{c1} K^0_S$ and $+1$ for $J/\psi K^0_L$. Due to the presence of even (L=0,2) and odd (L=1) orbital angular momenta in the $J/\psi K^{*0}(K^{*0} \to K^0_S \pi^0)$ system there can be *CP*-even and *CP*-odd contributions to the decay rate. When the angular information in the decay is ignored, the measured *CP* asymmetry in $J/\psi K^{*0}$ is reduced by a dilution factor $D_\perp = 1 - 2R_\perp$, where $R_\perp$ is the fraction of the L=1 component. It has been measured as $R_\perp = (16 \pm 3.5)\%$ which, after acceptance corrections leads to an effective $\eta_f = 0.65 \pm 0.07$ for this mode.

The B_{CP} and $B_{\rm flav}$ samples are used together in the unbinned maximum likelihood fit for the extraction of $\sin 2\beta$. A total of 45 parameters are varied in the fit, including $\sin 2\beta$ (1), the average mistag fraction w and the difference Δw between B^0 and $\overline{B}^0$ mistags for each tagging category (8), parameters for the signal Δt resolution (16) and parameters for background time dependence (9), Δt resolution (3) and mistag fractions (8). The determination of the mistag fractions and signal Δt resolution function is dominated by the large $B_{\rm flav}$ sample. Background parameters are governed by events with $m_{ES} < 5.27 \mathrm{GeV}/c^2$. As a result, the largest correlation between $\sin 2\beta$ and any linear combination of the other free parameters is only 0.13. The B lifetime and mixing frequency are fixed at $\tau_{B^0} = 1.548\,\mathrm{ps}$ and $\Delta M_{B^0} = 0.472\,\hbar\,\mathrm{ps}^{-1}$ respectively [7]. The value of $\sin 2\beta$ and the asymmetry in the Δt distribution were hidden using a blind analysis method (as described in [5]) until the event selection was optimized and all other aspects of the present analysis were complete.

Figure 2 shows the Δt distributions and A_{CP} as a function of Δt overlaid with the likelihood fit

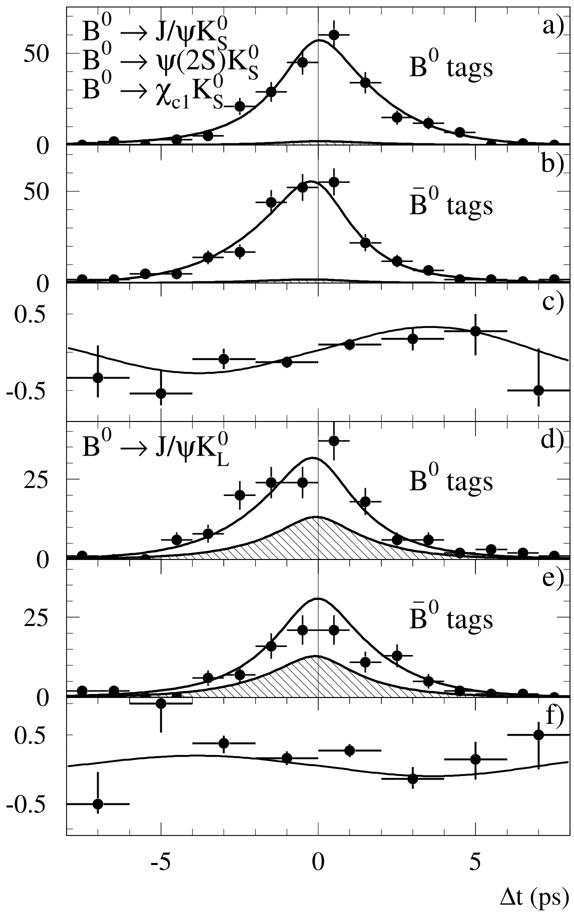

Figure 2. a) Number of $\eta_f = -1$ candidates in the signal region a) with a B^0 tag, N_{B^0} and b) with a $\overline{B}^0$ tag, $N_{\overline{B}^0}$ and c) the asymmetry $(N_{B^0} - N_{\overline{B}^0})/(N_{B^0} + N_{\overline{B}^0})$, as functions of Δt. The solid curves represent the result of the combined fit to all selected *CP* events and the shaded regions represent the background contributions. Figures d)-f) contain the corresponding information for the $\eta_f = +1$ mode. The likelihood is normalized to the total number of B^0 and $\overline{B}^0$ tags. The value of $\sin 2\beta$ is independent of the individual normalizations and therefore of the difference between the number of B^0 and $\overline{B}^0$ tags.

results for the $\eta_f = -1$ candidates. The probability of obtaining a lower likelihood value than the one from the fit, evaluated using a Monte Carlo technique, is 27%. The simultaneous fit to the full sample yields

$$\sin 2\beta = 0.59 \pm 0.14\,(\mathrm{stat}) \pm 0.05(\mathrm{syst}).$$

6.3. Systematic errors and consistency checks

The systematic error is dominated by the parametrization of the Δt resolution function (0.03) - due in part to residual uncertainties in SVT alignment, possible differences in the mistag fractions between the B_{CP} and B_{flav} samples (0.03) and uncertainties in the level, composition and *CP* asymmetry of the background in the selected *CP* events (0.02).

The large sample of reconstructed events allows a number of consistency checks, including separation of the data by decay mode, tagging category and B_{tag} flavour. The results of fits to these subsamples and to the samples of non-*CP* decay modes (where no statistically significant asymmetry is found) are shown in table 1.

7. Results from $B^0 \to \pi^+\pi^-, K^+\pi^-$ decays

A search for *CP*-violating asymmetries in decays of B^0 to two light mesons has been carried out on a sample of 33 million $B\overline{B}$ pairs [8]. Here one hopes to measure $\sin 2\alpha$ although the analysis is complicated by the possibility of penguin pollution leading to diagrams with different weak and strong phases contributing to the same final state. In this case, one has to allow for direct *CP* violation and in general $|\lambda| \neq 1$. The fit is then complicated by the presence of a cosine term as well as the coefficient of the sine term containing $\sin 2\alpha_{\mathrm{eff}}$, where α_{eff} depends on the magnitudes and strong phases of the tree and penguin amplitudes. The selected signal B sample consists of 65^{+12}_{-11} $\pi\pi$, 217 ± 18 $K\pi$ and $4.3^{+6.3}_{-4.3}$ KK events. The results for *CP*-violating asymmetries are summarized in table 3. Here $S_{\pi\pi}$ and $C_{\pi\pi}$ are respectively the coefficients of the sine and cosine terms in the expression for $\mathrm{f}_\pm(\Delta t)$ and

$$\mathcal{A}_{K\pi} \equiv \frac{N_{K^-\pi^+} - N_{K^+\pi^-}}{N_{K^-\pi^+} + N_{K^+\pi^-}}.$$

Figure 3 shows the Δt distributions and the asymmetry $\mathcal{A}_{\pi\pi}(\Delta t) = (N_{B^0}(\Delta t) - N_{\overline{B}^0}(\Delta t))/(N_{B^0}(\Delta t) + N_{\overline{B}^0}(\Delta t))$ for tagged events which are enhanced in signal $\pi\pi$ decays.

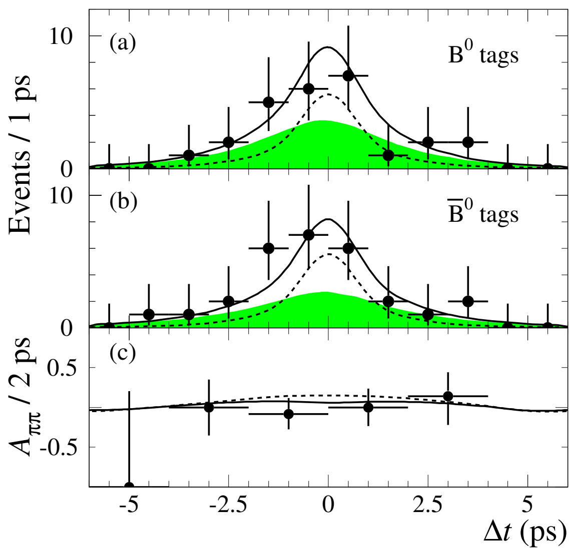

Figure 3. Distributions of Δt for events enhanced in signal $\pi\pi$ decays. Figures (a) and (b) show events (points with errors) with $B_{\rm tag} = B^0$ or $\overline{B}^0$. Solid curves represent projections of the maximum likelihood fit, dashed curves represent the sum of $q\overline{q}$ and $K\pi$ background events and the shaded region represents the contribution from signal $\pi\pi$ events. Figure (c) shows $\mathcal{A}_{\pi\pi}(\Delta t)$ for data (points with errors) as well as fit projections for signal and background events (solid curve) and signal events only (dashed curve).

8. Conclusions and outlook

The measurement of $\sin 2\beta$ presented here establishes *CP* violation in the B^0 meson system at the 4.1σ level, 37 years after its discovery in the Kaon system. The probability of obtaining this value of $\sin 2\beta$ or higher in the absence of *CP* violation is 3×10^{-5}. This direct measurement is consistent with the range implied by measurements and theoretical estimates of the magnitudes of CKM matrix elements [9]. By the summer of 2002, with a data sample of more than 100 million $B\overline{B}$ pairs a measurement of $\sin 2\beta$ with a precision of less than 0.1 will be possible.

In addition the search for *CP*-violating asymmetries in the decays $B^0 \rightarrow \pi^+\pi^-$ and $B^0 \rightarrow K^+\pi^-$ looks promising and with a similar amount of data should yield errors of ≈ 0.3 on the $B^0 \rightarrow \pi^+\pi^-$ asymmetries.

Table 3
Central values and 90% confidence level intervals for $S_{\pi\pi}$, $C_{\pi\pi}$ and $\mathcal{A}_{K\pi}$.

Parameter	Central Value	90% C.L. Interval
$S_{\pi\pi}$	$0.03^{+0.53}_{-0.56} \pm 0.11$	[-0.89,+0.85]
$C_{\pi\pi}$	$-0.25^{+0.45}_{-0.47} \pm 0.14$	[-1.0,+0.47]
$\mathcal{A}_{K\pi}$	$-0.07 \pm 0.08 \pm 0.02$	[-0.21,+0.07]

REFERENCES

1. J. H. Christenson, J. W. Cronin, V. L. Fitch and R. Turlay, Phys. Rev. Lett. **13** (1964) 138.
2. N. Cabibbo, Phys. Rev. Lett. **10** (1963) 531. M. Kobayashi and T. Maskawa, Prog. Theor. Phys. **49** (1973) 652.
3. B. Aubert *et al.* [BABAR Collaboration], SLAC-PUB-8569, hep-ex/0105044, to appear in Nucl. Instr. and Methods.
4. B. Aubert *et al.* [BABAR Collaboration], Phys. Rev. Lett. **87** (2001) 091801, hep-ex/0107013.
5. B. Aubert *et al.* [BABAR Collaboration], Phys. Rev. Lett. **86** (2001) 2515
6. See, for example L. Wolfenstein, Eur. Phys. J. C **15** (2000) 115.
7. D. E. Groom *et al.* [Particle Data Group Collaboration], Eur. Phys. J. C **15** (2000) 1.
8. B. Aubert *et al.* [BABAR Collaboration], hep-ex/0110062.
9. See, for example, F.J. Gilman, K. Kleinknecht and B. Renk, Eur. Phys. Jour. C **15**, 110 (2000).